Pramana – J. Phys. (2021) 95:37
https://doi.org/10.1007/s12043-020-02068-8

Microwave-assisted all-optical switching in a four-level atomic system

NGUYEN TUAN ANH[1], THAI DOAN THANH[1], NGUYEN HUY BANG[2] and HOANG MINH DONG[1],*

[1]Ho Chi Minh City University of Food Industry, Ho Chi Minh City, Vietnam
[2]Vinh University, 182 Le Duan Street, Vinh City, Vietnam
*Corresponding author. E-mail: dong.gtvtmt@gmail.com

MS received 1 June 2020; revised 27 October 2020; accepted 2 November 2020

Abstract. We study the all-optical switching of the weak probe field via a four-level atom system with the help of a microwave field and electromagnetically induced transparency effect. Here, the microwave field is used for coupling two-folded lower levels to which double dark resonances (DDRs) can arise. The atomic medium is switched from transparent to complete absorption under the DDRs. It is shown that the absorption spectrum, pulse propagations and all-optical switching dynamics of the probe field are dependent on the intensity of the microwave field, applied fields and probe detuning. Furthermore, the switching mode between the probe field and the microwave field can be antisynchronous or synchronous, depending on the probe detuning being adjusted to be equal to zero or $\pm\,\Omega_c$, respectively. Our results possibly are helpful in actual tests to design all-optical switching and optical storage devices in optical communications and signal processing.

Keywords. All-optical switching; microwave-assisted; electromagnetically induced transparency; double dark resonances.

PACS Nos **42.50.−p; 42.65.−k; 42.65.Pc; 42.90.+m**

1. Introduction

In the past several decades, atomic coherence and quantum interference have attracted tremendous interest in nonlinear and quantum optics fields due to its interesting effects and potential applications in quantum information systems and quantum computing [1–6]. Especially, electromagnetically induced transparency (EIT) [2,3] has tremendously attracted the attention the researchers because it can not only reduce the absorption of the medium but also modify the dispersion of the medium. The slow light forming due to the EIT can also enhance the interaction of light and matter significantly, which enhances nonlinear optical processes [7–20], such as nonlinear optics at low-light levels [7–9], slow-light group velocity [10], enhancement of Kerr nonlinearity [11–14], the creation of optical solitons propagation [15–20], and so on.

On the other hand, based on EIT, all-optical switching at low-light has also been extensively studied in recent years because it has favourable advantages compared to the conventional electro-optical switching, as high response speed and low switching thresholds. Harris and Yamamoto [21] first proposed a scheme of photon switching by quantum interference in a normal four-level N-type atomic system, in which switching of a single photon by another is achievable. Subsequently, Schmidt and Ram [22] proposed a way for the implementation of an all-optical switching, modulator and converter in a three-level system based on the EIT. Such switching can also be built up via the creation of dark states in a three-level system [23] and four-level system [24] in ion-doped crystals. Also, using a two-photon absorption scheme in an alkali-metal vapour cell, Yavuz [25] suggested a technique where a strong laser beam switches off another laser beam of different wavelengths in femtosecond time scales. Recently, based on the double-dark resonances (DDRs), all-optical switching was realised in a N-tripod five-level atom system [26]. Furthermore, DDRs in the EIT medium induced by the microwave field connecting to the fourth auxiliary energy level, which is known as the Autler–Townes effect also have been studied theoretically and experimentally [27,28]. In addition, a radiofrequency field

Published online: 15 February 2021

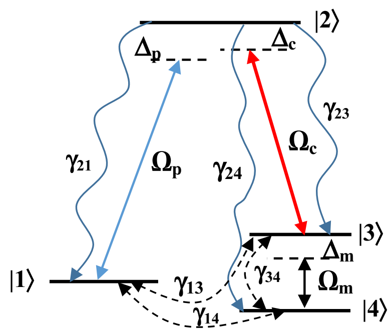

Figure 1. The four-level atomic scheme excited by two laser fields and a microwave field.

connects upper two-folded levels and DDRs can arise in a four-level cascade-type atomic medium (Yu and coworkers [29]). Most recently, some other low-light-level optical switching and bistability schemes have also been extensively investigated [30–34].

In this paper, the coherent control of pulse propagation and all-optical switching is investigated under the assistance of the microwave in a four-level atomic medium which consists of one excited level and three ground levels. By simultaneously solving the coupled Bloch–Maxwell equations for atom and field on numerical grids in time and space, we can control propagation dynamics and all-optical switching of the probe field through appropriately modulating the intensity of the two laser fields and the microwave field, and the probe detuning under the DDRs. The suggestions may be useful in the applications of all-optical switching or optical storage in optical communications.

2. Model and basic equations

We consider a four-level atomic system coupling by two laser fields and a microwave driving field as shown in figure 1, that comprises an excited state $|2\rangle$ and three ground states $|1\rangle$, $|3\rangle$ and $|4\rangle$. The transition $|2\rangle \leftrightarrow |3\rangle$ is driven by a coupling field with a carrier frequency of ω_c, and a one-half Rabi frequency $\Omega_c = \mu_{32}E_c/2\hbar$. A weak probe field with carrier frequency ω_p, and a one-half Rabi frequency $\Omega_p = \mu_{31}E_p/2\hbar$ is applied to the transition $|2\rangle \leftrightarrow |1\rangle$. The two ground levels $|3\rangle$ and $|4\rangle$ are coupled by a microwave field with carrier frequency ω_m and a one-half Rabi frequency $\Omega_m = \mu_{21}E_m/2\hbar$. Here $\mu_{ij} = \vec{\mu}_{ij}\hat{e}_L$ ($\hat{e}_L$ is the polarisation unit vector of the laser field) denotes the dipole moment for the transition between levels $|i\rangle$ and $|j\rangle$. The decay rates from the excited state $|2\rangle$ to the ground states $|1\rangle$, $|3\rangle$ and $|4\rangle$ are γ_{21}, γ_{23} and γ_{24}, respectively. Using the rotating-wave and the electric dipole approximations, the interaction Hamiltonian of the system in the interaction picture can be written as (by assuming $\hbar = 1$):

$$H_{\text{int}} = \begin{bmatrix} 0 & -\Omega_p & 0 & 0 \\ -\Omega_p^* & \Delta_p & -\Omega_c^* & 0 \\ 0 & -\Omega_c & \Delta_p - \Delta_c & -\Omega_m^* \\ 0 & 0 & -\Omega_m & \Delta_p - \Delta_c - \Delta_m \end{bmatrix}, \quad (1)$$

where $\Delta_p = \omega_{21} - \omega_p$, $\Delta_c = \omega_{23} - \omega_c$ and $\Delta_m = \omega_{34} - \omega_m$ are respectively detunings of the probe, coupling and microwave fields from the corresponding two-level transition frequencies.

Under the slowly-varying envelope, rotating wave and electric dipole approximations, the dynamics of the atom–field interaction for the microwave-driven four-level system is represented by the following coupled Bloch–Maxwell equations (in a retarded frame $\xi = z$ and $\tau = t - z/c$) [19]:

$$\frac{\partial\rho_{11}}{\partial\tau} = \gamma_{21}\rho_{22} - (\gamma_{13}+\gamma_{14})\rho_{11} + \gamma_{13}\rho_{33} + \gamma_{14}\rho_{44} + i\Omega_{p0}f^*(\xi,\tau)\rho_{21} - i\Omega_{p0}f(\xi,\tau)\rho_{12}, \quad (2a)$$

$$\frac{\partial\rho_{22}}{\partial\tau} = -(\gamma_{21}+\gamma_{23}+\gamma_{24})\rho_{22} + i\Omega_{p0}f(\xi,\tau)\rho_{12} - i\Omega_{p0}f^*(\xi,\tau)\rho_{21} + i\Omega_c^*\rho_{32} - i\Omega_c\rho_{23}, \quad (2b)$$

$$\frac{\partial\rho_{33}}{\partial\tau} = \gamma_{23}\rho_{22} + \gamma_{13}\rho_{11} + \gamma_{34}\rho_{44} - (\gamma_{13}+\gamma_{34})\rho_{33} + i\Omega_c^*\rho_{23} - i\Omega_c\rho_{32} + i\Omega_m^*\rho_{43} - i\Omega_m\rho_{34}, \quad (2c)$$

$$\frac{\partial\rho_{44}}{\partial\tau} = \gamma_{24}\rho_{22} + \gamma_{14}\rho_{11} + \gamma_{34}\rho_{33} - (\gamma_{14}+\gamma_{34})\rho_{44} + i\Omega_m^*\rho_{34} - i\Omega_m\rho_{43}, \quad (2d)$$

$$\frac{\partial\rho_{21}}{\partial\tau} = -\left(i\Delta_p + \frac{\gamma_{13}+\gamma_{14}+\gamma_{21}+\gamma_{23}+\gamma_{24}}{2}\right)\rho_{21} - i\Omega_{p0}f(\xi,\tau)(\rho_{22}-\rho_{11}) + i\Omega_c^*\rho_{31}, \quad (2e)$$

$$\frac{\partial\rho_{31}}{\partial\tau} = -\left(\gamma_{13} + \frac{\gamma_{14}}{2} + \frac{\gamma_{34}}{2} + i(\Delta_p - \Delta_c)\right)\rho_{31} - i\Omega_{p0}f(\xi,\tau)\rho_{32} + i\Omega_c\rho_{21} + i\Omega_m\rho_{41}, \quad (2f)$$

$$\frac{\partial\rho_{41}}{\partial\tau} = -\left(\gamma_{14} + \frac{\gamma_{13}}{2} + \frac{\gamma_{34}}{2} + i(\Delta_p - \Delta_c - \Delta_m)\right)\rho_{41} + i\Omega_{p0}f(\xi,\tau)\rho_{24} + i\Omega_m\rho_{31}, \quad (2g)$$

$$\frac{\partial\rho_{32}}{\partial\tau} = -\left(\frac{\gamma_{13}+\gamma_{34}+\gamma_{21}+\gamma_{23}+\gamma_{24}}{2} - i\Delta_c\right)\rho_{23} - i\Omega_c(\rho_{33}-\rho_{22}) - i\Omega_m^*\rho_{24}, \quad (2h)$$

$$\frac{\partial\rho_{42}}{\partial\tau} = -\left(\frac{\gamma_{14}+\gamma_{34}+\gamma_{21}+\gamma_{23}+\gamma_{24}}{2} + i(\Delta_c + \Delta_m)\right)\rho_{42} - i\Omega_{p0}f(\xi,\tau)\rho_{41} - i\Omega_c^*\rho_{43} + i\Omega_m\rho_{32}, \quad (2i)$$

$$\frac{\partial\rho_{34}}{\partial\tau} = -\left(\gamma_{34} + \frac{\gamma_{13}}{2} + \frac{\gamma_{14}}{2} + i\Delta_p\right)\rho_{34}$$

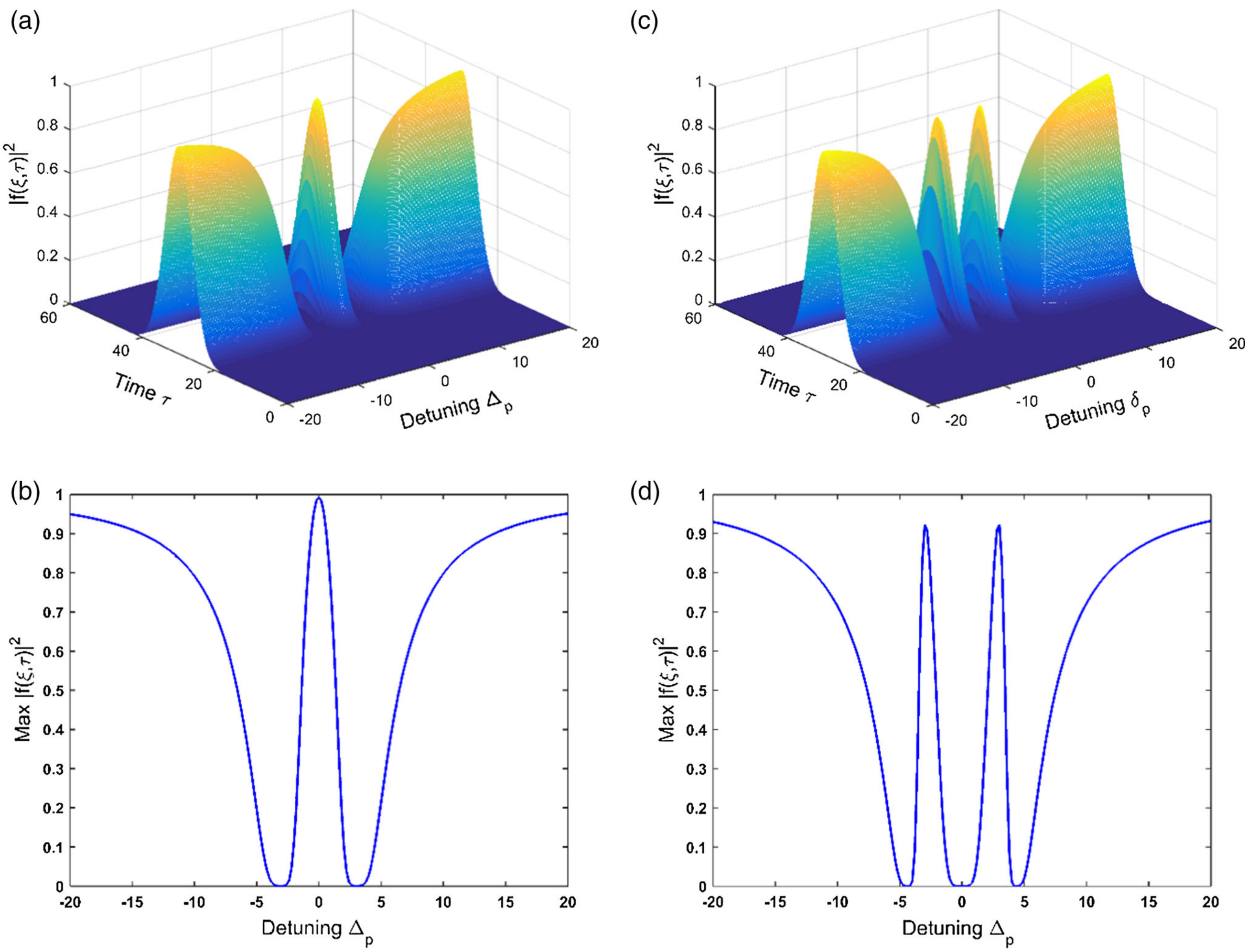

Figure 2. The influences of the microwave field and the detuning Δ_p on the probe absorption spectra in the absence and presence of the microwave field: $\Omega_m = 0$ (for panels (**a**) and (**b**)) and $\Omega_m = 3\gamma_{21}$ (for panels (**c**) and (**d**)). Other parameters are chosen as $\Omega_{p0} = 0.01\gamma_{21}$, $\Omega_c = 3\gamma_{21}$, $\Delta_c = \Delta_m = 0$, $\xi = 100/\alpha$, respectively.

$$+i\Omega_m(\rho_{44} - \rho_{33}) + i\Omega_c^*\rho_{24}. \tag{2j}$$

$$\frac{\partial f(\xi,\tau)}{\partial(\alpha\xi)} = i\frac{\gamma_{21}}{\Omega_{p0}}\rho_{21}(\xi,\tau). \tag{2k}$$

Here,

$$\alpha = \frac{\omega_p N |d_{21}|^2}{4\varepsilon_0 c\hbar\gamma_{21}},$$

is the propagation constant. In the following, we numerically solve eqs (2a)–(2k) on a space–time grid by fourth-order Runge–Kutta and finite difference method. The computer code developed for this problem is an expansion of our previous work [19,34]. We assumed that the initial conditions in all the atoms start in the ground state $|1\rangle$ and the boundary condition assumed by the probe field is a Gaussian-type pulsed $f(\xi = 0, \tau) = \exp[-(\ln 2)(\tau - 30)^2/\tau_0^2]$, with $\tau_0 = 6/\gamma_{21}$ the temporal width of the Gaussian pulse at the beginning on the medium.

3. Results and discussion

To illustrate the applications of the model, we apply the cold atomic medium of ^{87}Rb on the $5S$–$5P$ transitions as a realistic candidate. The designated states can be chosen as follows: $|1\rangle = |5S_{1/2}, F = 2, m_F = 2\rangle$, $|2\rangle = |5P_{3/2}, F = 2, m_F = 1\rangle$, $|3\rangle = |5S_{1/2}, F = 2, m_F = 0\rangle$, $|4\rangle = |5S_{1/2}, F = 1, m_F = 0\rangle$, and assume that the decay rates from the excited level $|2\rangle$ to the three ground levels are $\gamma_{21} = \gamma_{23} = \gamma_{24} = 2\pi \times 5.9$ MHz, the non-radiative decay rates between the three ground levels are $\gamma_{13} = \gamma_{14} = \gamma_{34} = 0.01\gamma_{21}$, and wavelength of the probe, coupling lasers $\lambda = \lambda_c = 780$ nm, [35], respectively. For simplicity, all quantities related to the frequency are scaled by γ_{21}, which should be of the order of MHz for rubidium sodium atoms.

First of all, we consider the influences of the microwave field and detuning Δ_p on the absorption properties of the probe field. Figures 2a and 2c show the pulse at the end of the propagation process as a function of time τ and detuning Δ_p, whereas figures 2b and 2d demonstrate the maximal value of the function $|f(\xi,\tau)|^2$ at the end of the propagation process as a function of detuning Δ_p, under the resonant condition $\Delta_c = \Delta_m = 0$, in the absence and presence of the microwave field Ω_m. As shown in figure 2, the absorption spectra of the probe field depend so sensitively on the turn-on and turn-off of the microwave field. Specifically, when no microwave field is applied ($\Omega_m = 0$, see figures 2a and 2b), the absorption of the probe field can be suppressed and the atomic medium becomes transparent to the weak probe field at the line centre. When the microwave field is turned on ($\Omega_m = \Omega_c = 3\gamma_{21}$, see figures 2c and 2d), the medium is switched from transparent to complete absorbing at the line centre, i.e. has an electromagnetically induced absorption (EIA). Furthermore, the envelope of the maximal value $|f(\xi,\tau)|^2$ at the two largest absorbed probe field positions are converted into two non-absorbed probe field positions $\Delta_p = \pm\Omega_c$, respectively.

In order to get a deeper insight into the dependence of the envelope of the maximal value $|f(\xi,\tau)|^2$ of the probe field on the microwave field strength Ω_m at the central and side-band peaks, we plot the variation of both the central peak (blue solid line: $\Delta_p = 0$) and two side-band peaks (red dashed line: $\Delta_p = \pm\Omega_c$), as shown in figure 3. When $\Delta_p = 0$, we find that the magnitude of the probe absorption first increases rapidly from zero with the increase of the microwave field strength from 0 to a maximal value $3\gamma_{21}$ and then reaches the steady-state value when the strength of the microwave field continuously increases. In contrast, when $\Delta_p = \pm\Omega_c = \pm 3\gamma_{21}$ the magnitude of the probe absorption decreases from a maximal to zero at $\Omega_m = 3\gamma_{21}$, and then increases to a value larger than zero and finally tends to a small steady-state value.

In figure 4, we plot the temporal evolution of the normalised probe pulse envelope $|f(\xi,\tau)|^2$ at the beginning ($z = 0$), as shown in figure 4a and the exit of the medium (figures 4b, $\xi = 20/\alpha$ and 4c, $\xi = 50/\alpha$) under of the coupling field intensity $\Omega_c = 3\gamma_{21}$ by modulating the intensity of the microwave field values, $\Omega_m = 0, 0.5\gamma_{21}, 1\gamma_{21}, 2\gamma_{21}$ and $3\gamma_{21}$, respectively. It can clearly be seen from figure 4 that the turn-off and on of the microwave field significantly affect the amount of probe pulse absorption during the propagation in the four-level atomic medium. With a gradual increase of the microwave field strengths, it is apparent that the absorption of the probe pulse increases considerably. Specifically, when the microwave field is switched off (i.e. $\Omega_m = 0$), the probe pulse is transmitted almost without losses and the atomic medium is transparent to the probe pulse after a characteristic propagation length. Moreover, the pulse shape remains Gaussian during propagation. In contrast, when $\Omega_m \neq 0$, i.e., when the microwave field is switched on, the probe pulse is absorbed obviously at the exit of the medium. In addition, it can easily be seen from figures 4b and

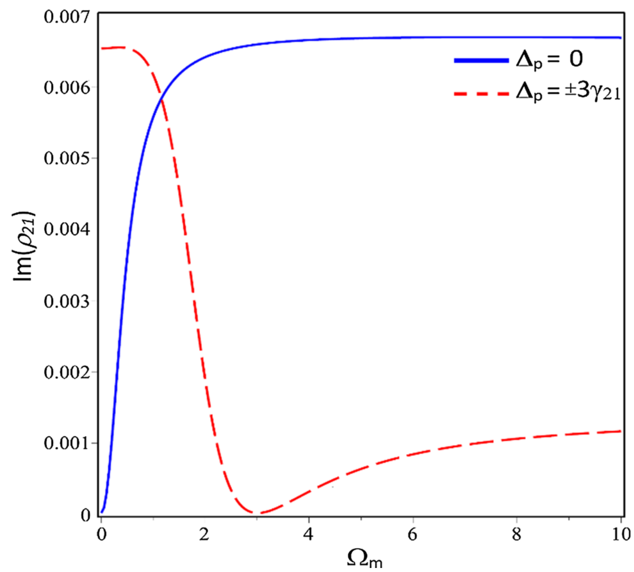

Figure 3. The variation of probe absorption vs. microwave field strength when $\Delta_p = 0$ (blue solid line) and $\Delta_p = \pm 3\gamma_{21}$ (red dashed line). Other parameters are the same as in figure 2.

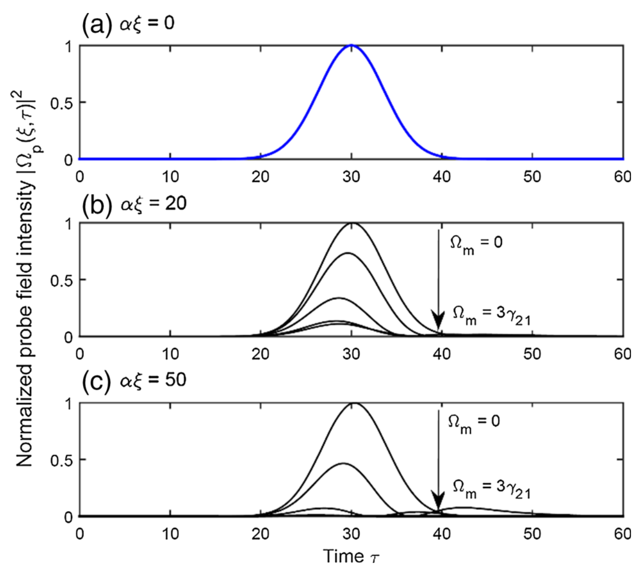

Figure 4. Magnitude squared of probe pulse envelopes at the entrance to the medium $\xi = 0$ (**a**), the exit of the medium $\xi = 20/\alpha$ (**b**) and $\xi = 50/\alpha$ (**c**) for five different values of the microwave field strength (from the top curve to the bottom curve corresponding to the small value to the large value: $\Omega_m = 0, 0.5\gamma_{21}, 1\gamma_{21}, 2\gamma_{21}$ and $3\gamma_{21}$, respectively) under the condition of the control field intensity $\Omega_c = 3\gamma_{21}$. Other parameters are $\tau_0 = 6/\gamma_{21}$, $\Omega_{p0} = 0.01\gamma_{21}$, $\Delta_p = \Delta_c = \Delta_m = 0$, respectively.

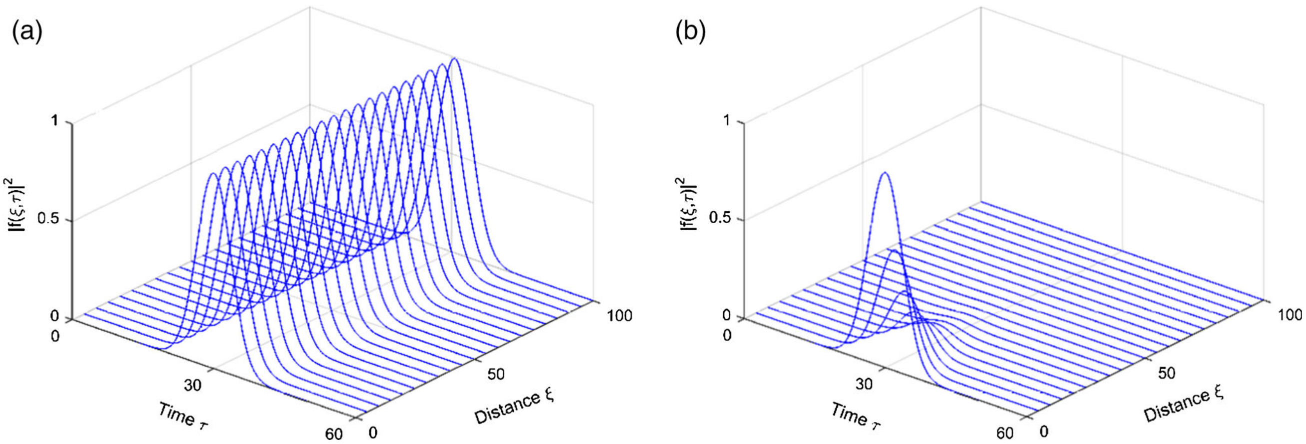

Figure 5. The space–time evolution of the normalised probe field intensity for the switch-off and switch-on of the microwave field. (**a**) $\Omega_m = 0$ and (**b**) $\Omega_m = 3\gamma_{21}$. Other parameters are $\Omega_{p0} = 0.01\gamma_{21}$, $\Omega_c = 3\gamma_{21}$, $\Delta_p = \Delta_c = \Delta_m = 0$, respectively.

4c that increasing the value of the microwave field strength leads to a gradual increase in the probe pulse absorption, as seen in figure 3. When the strength of the microwave field increases further to a higher value (e.g. $\Omega_m = \Omega_c = 3\gamma_{21}$), evidently the probe pulse is strongly attenuated and will be completely absorbed by the atomic medium in a characteristic propagation distance. As a result, by suitably tuning the microwave field, we can realise all-optical modulation for such probe pulsed light.

To illustrate explicitly the above analysis, we present the spatiotemporal evolution of the magnitude squared of the normalised probe pulse envelope in the two cases $\Omega_m = 0$ (switching microwave field off) and $\Omega_m = 3\gamma_{21}$ (switching microwave field on), and we display three-dimensional plots in figure 5 for the control field intensity $\Omega_c = 3\gamma_{21}$. The figures show that the probe pulse can propagate with almost transparency and still can preserve their shapes over long distances in the absence of the microwave field as shown in figure 5a. When the microwave field is applied ($\Omega_m = 3\gamma_{21}$), the probe pulse can be completely absorbed by the medium in a very short propagation distance (see figure 5b). These results are consistent with the absorption spectral profile of the probe field given in figures 2 and 3 as well as the comments in figure 4.

Next, we investigate the effect of probe detuning on the spatiotemporal evolutions of the normalised probe pulse envelope. By adjusting the value of the probe frequency detuning Δ_p, we find that the propagation of the probe pulse and the shape of the probe pulse are changed. When the probe detuning increases gradually, it can be found that the pulse gradually achieves lossless propagation (see figures 6a–6c). That is, when $0 < \Delta_p \leq 3\gamma_{21}$, the absorption of the probe pulse becomes smaller and can be ignored completely, when $\Delta_p = 3\gamma_{21}$, propagation of the probe pulse without attenuation can be formed (see figure 6c). When $\Delta_p > 3\gamma_{21}$, the absorption of the probe pulse becomes large so that propagation of the probe pulse is strongly attenuated as shown in figure 6d.

Finally, we consider the dynamics of the possible switching process of the probe field propagating through the four-level atomic medium (shown in figure 7). Here, the time evolution for the weak probe field is assumed to be a continuous wave and the switching microwave field a nearly-square pulse with smooth rising and falling edges. Here, the switching microwave field $\Omega_m(\tau) = \Omega_{m0}\{1 - 0.5\tanh[0.4(\tau - 20)] + 0.5\tanh[0.4(\tau - 45)] - 0.5\tanh[0.4(\tau - 70)] + 0.5\tanh[0.4(\tau - 95)]\}$, which is normalised by its peak value $\Omega_{m0} = 3\gamma_{21}$, is turned on or off at an approximate period of $50/\gamma_{21}$. In figure 7, we see the time evolution of a weak probe field is (red dashed lines) and the switching microwave field (blue solid line) at the propagation distance $\xi = 100/\alpha$. As shown in figure 7, the probe transmission is switched to a nearly-square pulse train depending on the ON or OFF mode of the microwave field and frequency detuning of the probe field. Indeed, when $\Delta_p = 0$, the probe intensity is switched antisynchronously with the modulation mode of the microwave field (figure 7a). However, when $\Delta_p = 3\gamma_{21}$, the probe is switched synchronously with the microwave field (figure 7b). This behaviour can be explained by noting that the absence or presence of the microwave field can switch respectively the medium to a transparent or strong absorptive mode due to DDRs. Consequently, this four-level atomic system can be used for the realisation of an all-optical switching of the weak probe field by the modulation of the microwave field.

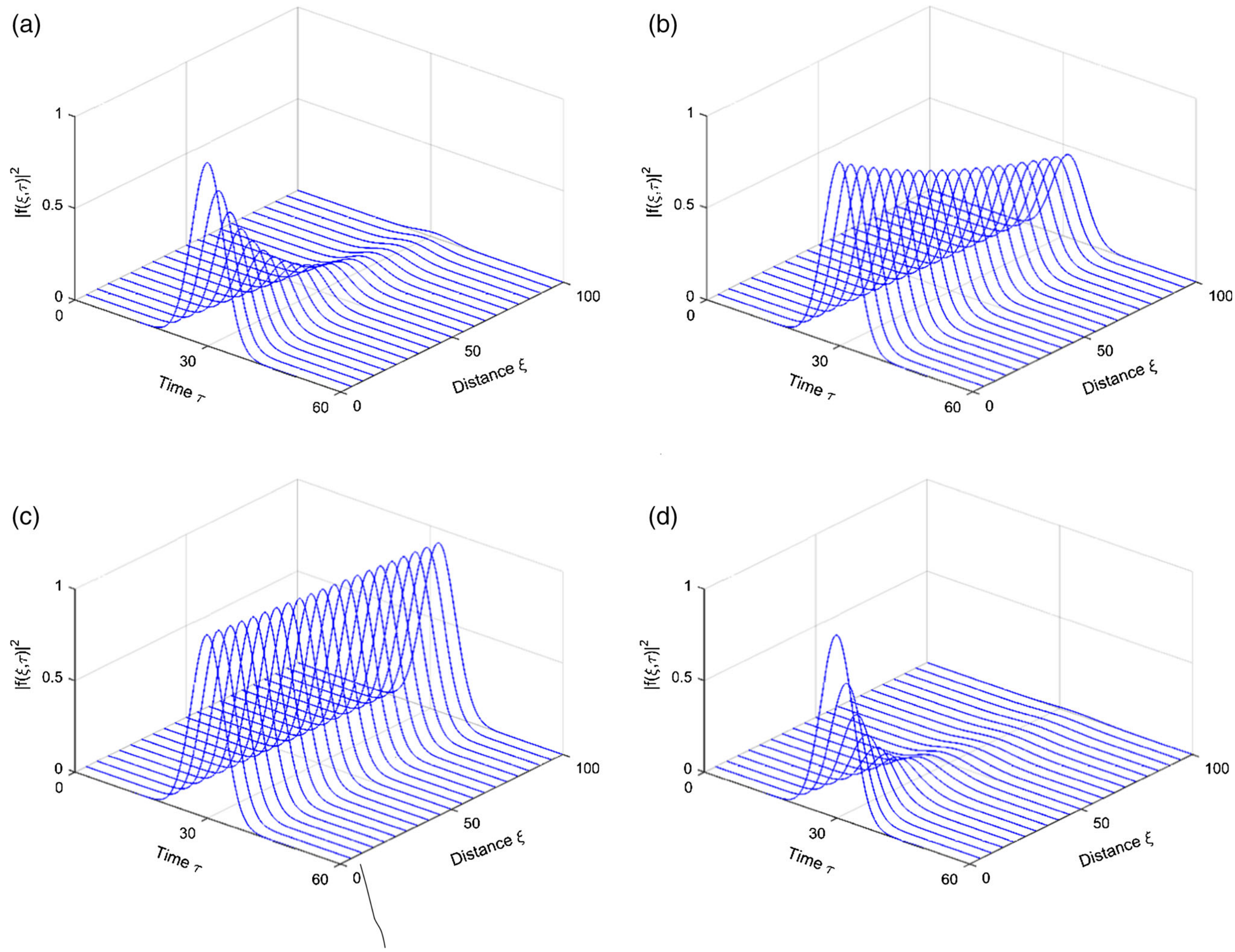

Figure 6. The space–time evolution of the normalised probe field intensity for the switch-on and switch-off of the microwave field. (**a**) $\Delta_p = 1\gamma_{21}$, (**b**) $\Delta_p = 2\gamma_{21}$, (**c**) $\Delta_p = 3\gamma_{21}$ and (**d**) $\Delta_p = 4\gamma_{21}$. Other parameters are $\Omega_{p0} = 0.01\gamma_{21}$, $\Omega_c = 3\gamma_{21}$, $\Omega_m = 3\gamma_{21}$, $\Delta_c = \Delta_m = 0$, respectively.

4. Possible experimental realisation

In this section, we provide a possible realisation of all-optical switching in the microwave-driven four-level cold ^{87}Rb atoms system. The excitation scheme and experimental arrangement can be similar to that described in ref. [36]. Here, the states $|1\rangle$, $|3\rangle$, $|4\rangle$ and $|2\rangle$ are given as $5S_{1/2}$ ($F = 2$, $m_F = 2$), $5S_{1/2}$ ($F = 2$, $m_F = 0$), $5S_{1/2}$, ($F = 1$, $m_F = 0$) and $5P_{3/2}$ ($F = 2$, $m_F = 1$), respectively. In this choice, both the probe field and the coupling field can be used by a combination of a single-mode external cavity diode laser (780 nm) and an acousto-optic modulator (AOM). The coupling and the probe fields are circularly polarised with the right (σ^+ polarisation) and left (σ^- polarisation) helicities, respectively. A 6.84 GHz microwave drives the magnetic-dipole transition between two hyperfine ground states $5S_{1/2}$ ($F = 2$, $m_F = 0$) and $5S_{1/2}$ ($F = 1$, $m_F = 0$) [35].

5. Conclusion

We have studied the propagation dynamics and all-optical switching of a weak probe pulse in a four-level atomic system under the influence of the microwave field. It is shown that the probe absorption depends sensitively on the turn ON or turn OFF of the microwave field and frequency detuning of the probe field. By choosing the parameters appropriately, the probe pulse may propagate without loss over a long distance when the microwave field is absent. In contrast, when the microwave field is present, the probe pulse can be completely absorbed in a short propagation distance. Also,

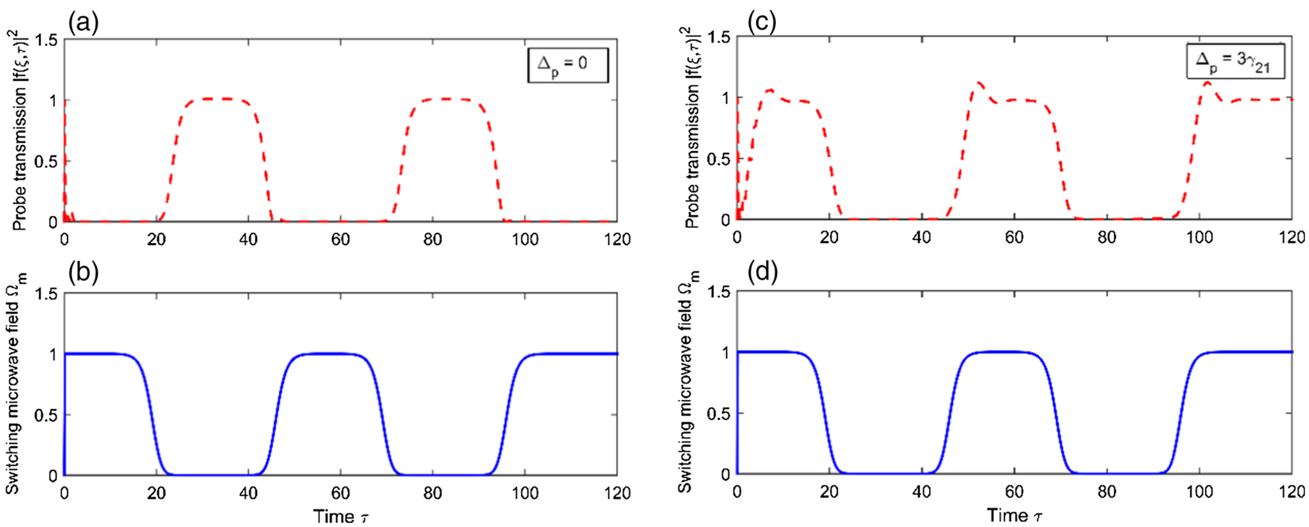

Figure 7. Time evolution of a cw probe field (red dashed line) at $\xi = 100/\alpha$ when the microwave field (blue solid line) switched at period $50/\gamma_{21}$, for different values of the probe frequency detuning: ((**a**), (**b**)) $\Delta_p = 0$ and ((**c**), (**d**)) $\Delta_p = 3\gamma_{21}$. Other parameters are $f(\xi = 0, \tau) = 1$, $\Omega_{p0} = 0.01\gamma_{21}$, $\Omega_c = 3\gamma_{21}$, $\Omega_{m0} = 3\gamma_{21}$, $\Delta_c = \Delta_m = 0$, respectively.

we obtain once again a stable pulse propagation when the frequency detuning $\Delta_p = \pm\Omega_c$, corresponding to the two side-band peaks of the DDRs. Furthermore, we also show that the switching mode relies on the control of the DDRs which appear in the system, the probe pulse is switched antisynchronously or synchronously with the switching of the microwave field at the central or two side-band peaks of the probe absorption spectra, respectively. Our results provide a guideline for optimising and controlling the optical switching operations in a four-level atomic system which is suitable for realising all-optical switching or optical storage devices working at low light levels.

Acknowledgements

This work has been sponsored and funded by Ho Chi Minh City University of Food Industry under Contract Nos. 148/HD-DCT and 62/HD-DCT.

References

[1] H Ishikawa, *Ultrafast all-optical signal processing devices* (Wiley, 2008) Chapters 1, 2, https://onlinelibrary.wiley.com/doi/book/10.1002/9780470758694.
[2] A Imamoglu and S E Harris, *Opt. Lett.* **14**, 1344 (1989)
[3] K J Boller, A Imamoglu and S E Harris, *Phys. Rev. Lett.* **66**, 2593 (1991)
[4] S E Harris, *Phys. Today* **50**, 36 (1997)
[5] M Fleischhauer, A Imamoglu and J P Marangos, *Rev. Mod. Phys.* **77**, 633 (2005)
[6] Chun-Liang Wang and Yan-Li Meng, *Opt. Commun.* **285**, 2632 (2012)
[7] S E Harris and L V Hau, *Phys. Rev. Lett.* **82**, 4611 (1999)
[8] B-W Shiau, M-C Wu, C-C Lin and Y-C Chen, *Phys. Rev. Lett.* **106**, 193006 (2011)
[9] V Venkataraman, K Saha and A L Gaeta, *Nat. Photon.* **7**, 138 (2013)
[10] L V Hau, S E Harris, Z Dutton and C H Bejroozi, *Nature* **397**, 594 (1999)
[11] H Schmidt and A Imamoglu, *Opt. Lett.* **21**, 1936 (1996)
[12] C J Zhu, C Hang and G X Huang, *Eur. Phys. J. D* **56**, 231 (2010)
[13] D X Khoa, L V Doai, D H Son and N H Bang, *J. Opt. Soc. Am. B* **31**, 1330 (2014)
[14] H R Hamedi, A H Gharamaleki and M Sahrai, *Appl. Opt.* **22**, 5892 (2016)
[15] G Huang, K Jiang, M G Payne and L Deng, *Phys. Rev. E* **73**, 056606 (2006)
[16] L G Si, X-Y Lü, X-Y Hao and J-H Li, *J. Phys. B At. Mol. Opt. Phys.* **43**, 065403 (2010)
[17] H M Dong, L V Doai, V N Sau, D X Khoa and N H Bang, *Photon. Lett. Pol.* **8**, 73 (2016), http://photonics.pl/PLP/index.php/letters/article/view/667.
[18] D X Khoa, H M Dong, L V Doai and N H Bang, *Optik* **131**, 497 (2017)
[19] H M Dong, L V Doai and N H Bang, *Opt. Commun.* **426**, 553 (2018)
[20] H M Dong, L T Y Nga, D X Khoa and N H Bang, *Sci. Rep.* **10**, 15298 (2020)
[21] S E Harris and Y Yamamoto, *Phys. Rev. Lett.* **81**, 3611 (1998)
[22] H Schmidt and R J Ram, *Appl. Phys. Lett.* **76**, 3173 (2000)
[23] B S Ham, *J. Mod. Opt.* **49**, 2477 (2002)
[24] S A Moiseev and B S Ham, *Phys. Rev. A* **73**, 033812 (2006)

[25] D D Yavuz, *Phys. Rev. A* **74**, 053804 (2006)
[26] M A Antón, F Carreño, O G Calderón, S Melle and I Gonzalo, *Opt. Commun.* **281**, 6040 (2008)
[27] L J Yang, L S Zhang, X L Li, L Han, G S Fu, N B Manson, D Suter and C J J Wei, *Phys. Rev. A* **72**, 053801 (2005)
[28] Z J Du, S G Zhang, C J Wu, Y Guan, W Y Zhao and H Chang, *Chin. Phys. Lett.* **27**(**10**), 104202 (2010)
[29] R Yu, J Li, P Huang, A Zheng and X Yang, *Phys. Lett. A* **373**, 2992 (2009)
[30] J H Li, R Yu and Y Wu, *J. Appl. Phys.* **113**, 103104 (2013)
[31] H R Hamedi, *Laser Phys.* **27**, 066002 (2017)
[32] H Jafarzadeh, *Laser Phys.* **27**, 025204 (2017)
[33] H M Dong, L T Y Nga and N H Bang, *Appl. Opt.* **58**, 4192 (2019)
[34] H M Dong and N H Bang, *Phys. Scr.* **94**, 115510 (2019)
[35] D Steck, https://steck.us/alkalidata
[36] Y-C Chen, Y-A Liao, H-Y Chiu, J-J Su and I A Yu, *Phys. Rev. A* **64**, 053806 (2001)